Highly Nonexponential Kinetics in the Early-Phase Refolding of Proteins at Low Temperatures

Satoshi Saigo* and Naoya Shibayama

Division of Biophysics, Department of Physiology, Jichi Medical School, Minamikawachi, Tochigi 329-0498, Japan

Received March 25, 2003; Revised Manuscript Received June 23, 2003

ABSTRACT: Theory and simulations predict that the folding kinetics of protein-like heteropolymers become nonexponential and glassy (i.e., controlled by escape from different low-energy misfolded states) at low temperatures, but there was little experimental evidence for such behavior of proteins. We have developed a stopped-flow instrument working reliably down to −40 °C with high mixing capability and applied it to study the refolding kinetics of horse cytochrome *c* (cyt *c*) and hen egg white lysozyme at temperatures below 0 °C in the presence of antifreeze NaCl, LiCl, or ethylene glycol and above 0 °C in the presence and absence of antifreeze. The refolding was initiated by rapid dilution of the guanidine hydrochloride unfolded proteins, and the kinetics were monitored by intrinsic tryptophan fluorescence. Highly nonexponential kinetics extended over 3 decades in time (0.01−10 s) were observed in the early phases of the refolding of cyt *c* and lysozyme in the temperature range of −35 to 5 °C. These results are in agreement with the theoretical prediction, suggesting that the folding energy landscapes of these proteins are rugged in the upper portions.

A polypeptide chain folds to its unique native conformation in a biologically relevant time despite the huge number of all possible conformations (the Levinthal paradox) (*1*). The paradox is solved theoretically by taking a "new view" (*2*, *3*) in which proteins fold from a large ensemble of unfolded conformations to the native conformations, forming parallel trajectories running down on energy landscapes shaped like a funnel. This view emphasizes the ruggedness of the landscape and the heterogeneity of the folding ensemble. Indeed, theory (*2*, *4*) and simulations (*5*, *6*) predict that the kinetics of protein folding become nonexponential and glassy (i.e., dominated by escape from different low-energy misfolded states) at low temperatures. Gillespie and Plaxco (*7*) tried to detect such nonexponential behavior in the refolding kinetics of a small single-domain protein, protein L, in the presence of ethylene glycol as antifreeze but only found that the kinetics are strictly exponential down to −15 °C. Gruebele and co-workers (*8*) observed that the refolding kinetics of cold-denatured forms of two proteins, phosphoglycerate kinase and a ubiquitin mutant, are nonexponential at near room temperature, but they also found that the kinetics become exponential at lower temperatures, inconsistent with theoretical expectation of the glassy behavior of refolding proteins. Observation of the glassy nonexponential behavior of proteins provides a unique opportunity to assess the correspondence between theory and experiment and is of particular importance because it allows evaluation of how truly optimized for folding the proteins are (*4*, *6*).

A difficulty in exploring the kinetics of protein refolding is that its early stages often occur in a burst phase that is completed within the dead time (2−5 ms) of the stopped-flow method, the most powerful and versatile technique for studying the kinetics of protein refolding. The amplitudes of this phase, however, can be detected by stopped-flow experiments monitoring fluorescence, far-UV circular dichroism (CD),[1] and small-angle X-ray scattering (*9*, *10*). These experiments have shown that in many medium-sized single-domain proteins, consisting of more than 100 residues, a transient compact intermediate accumulates during this phase. The intermediate resembles a molten globule that is characterized by some nativelike secondary structure and chain topology without tight packing of the side chains (*9*−*11*). This raises the possibility that the early folding events are crucial for directing unfolded proteins roughly but efficiently toward their native topologies.

In the present study, we used a low-temperature stopped-flow method (*12*) and characterized the burst phases of the refolding of two proteins, horse heart ferric cytochrome *c* (cyt *c*) and hen egg white lysozyme. Highly extended nonexponential kinetics were observed in the early phases of the refolding at low temperatures and are interpreted in terms of heterogeneous glassy kinetics exhibited by the refolding polypeptides.

MATERIALS AND METHODS

Construction of a Low-Temperature Stopped-Flow Instrument. A low-temperature stopped-flow instrument, basically the same in its design as the model of Van Wart and Zimmer (*13*) but with several modifications and improvements as described below, was constructed in collaboration with Unisoku, Osaka. Sample reservoirs are connected to driving

* To whom correspondence should be addressed. Tel: (285)-58-7307. Fax: (285)-40-6294. E-mail: saigos@jichi.ac.jp.

[1] Abbreviations: CD, circular dichroism; cyt *c*, cytochrome *c*; GdnHCl, guanidine hydrochloride; 8-Hq, 8-hydroquinoline; Hepes, *N*-(2-hydroxyethyl)piperazine-*N*′-2-ethanesulfonic acid.

10.1021/bi034484y CCC: $25.00
Published on Web 07/23/2003

syringes and the syringes to a mixer through ruby-ball valves (*14*) for ensuring leak-free pathway selection at temperatures down to −40.0 °C. The mixer is of a three-stage four-jet type, which accomplishes efficient mixing of solutions of high viscosities. An observation cell, made from a quartz capillary tube, is of 2 mm path length for fluorescence excitation and emission. A 150 W Hg−Xe arc lamp (L7047; Hamamatsu Photonics) and an interference filter (03FIM018; Melles Griot) provided the excitation of tryptophan at 280 nm; the emission at 90° was detected above 325 nm with a cutoff filter and photomultiplier. Signals were sampled at equal intervals on a logarithmic time scale and averaged 10−30 times using stopped-flow data acquisition software (TSPL-5; Unisoku, Osaka). The performance characteristics of the instrument approximately met the criteria of Auld (*12*). In particular, the temperature of the stopped-flow module was controlled uniformly within ±0.2 °C by means of a low-temperature bath circulator (ULT-80DD; Neslab).

Refolding Measurements. Horse heart cyt *c* (type IV) was purchased from Sigma and hen egg white lysozyme (six times crystallized) from Seikagaku Kogyo, Tokyo, and they were used without further purification. Imidazole (purity >99%) was obtained from Aldrich and twice crystallized to remove fluorescent impurities. Ultrapure guanidine hydrochloride (GdnHCl) Bio-34 was purchased from Nakarai, Osaka. Buffers for cyt *c* refolding were prepared by mixing 6.0 M GdnHCl in the buffer (0.1 M imidazole, pH 6.5) with 4.5 M NaCl in the buffer or 2.0 M GdnHCl and 4.3 M LiCl in the buffer with 5.5 M LiCl in the buffer in appropriate volume ratios to yield final variable GdnHCl concentrations. Buffers for lysozyme refolding were prepared similarly by mixing 5.5 M GdnHCl and 0.38 M NaCl in the buffer (50 mM sodium cacodylate, pH 6.5) with 4.5 M NaCl in the buffer, 5.6 M GdnHCl in the buffer with 35% (v/v) ethylene glycol in the buffer, or 6.0 M GdnHCl in the buffer (70 mM NaCl, pH 1.5) with the buffer. The unfolded proteins were mixed with 6 volumes of refolding buffers of variable GdnHCl concentrations in the stopped-flow instrument, and the refolding kinetics were measured by monitoring the tryptophan fluorescence changes. The equilibrium unfolding curves of the proteins were also obtained on the stopped-flow instrument by measuring their fluorescence at different GdnHCl concentrations. The protein solutions for low-temperature measurements were incubated beforehand for 30 min at 25 °C, for over 1 h at −20 °C, and for 20 min at measuring temperatures for ensuring thermal equilibration.

Viscosity Measurements. An Ubbelohde viscometer (No. 72312; Shibata, Tokyo) having an out-flow time of about 200−500 s was filled with sample solutions and immersed in a methanol bath of the low-temperature circulator. Their viscosities were measured after thermal equilibration. The viscometer was calibrated in the temperature range of 10 to −30 °C using a 30 wt % $CaCl_2$ aqueous solution as a standard.

RESULTS

Low-Temperature Stopped-Flow Measurements. A fluorescence stopped-flow instrument working reliably at temperatures down to −40 °C and allowing efficient mixing of solutions with viscosities up to 25 cP (1 cP = 1 mPa s) was developed and used for kinetic measurements. In most cases, concentrated neutral salts such as NaCl and LiCl rather than organic solvents such as methanol and ethylene glycol were used as antifreeze. This is because the viscosities of these salt solutions are relatively low even at low temperature (*15*), which is essential for efficient mixing of solutions.

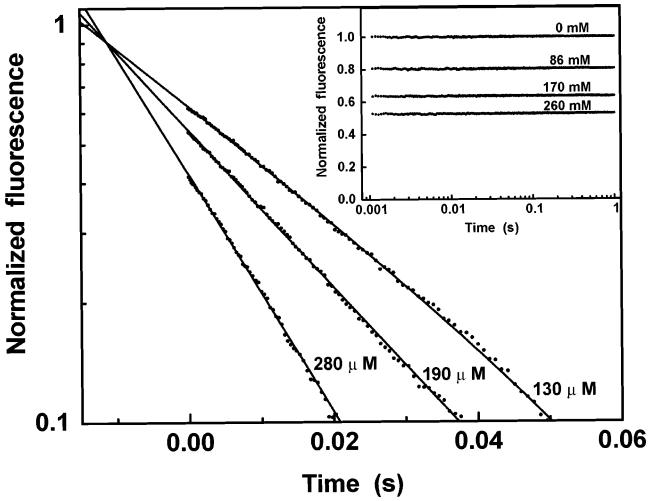

FIGURE 1: Performance characteristics of the low-temperature stopped-flow instrument. The dead time was estimated by probing the binding of 8-Hq to Zn^{2+} under the same solvent conditions as used in the refolding experiments on cyt *c* at −35 °C. 100 μM 8-Hq in the buffer (0.1 M Tris, pH 6.5) containing 1.5 M GdnHCl and 4.6 M LiCl was mixed at −35 °C with 6 volumes of variable concentrations of $ZnCl_2$ in the buffer containing 5.5 M LiCl. The fluorescence of the Zn^{2+} complex was excited at 360 nm and detected above 425 nm. Fluorescence changes after mixing are shown as semilogarithmic plots. The final Zn^{2+} concentrations are shown at the upside of each curve. The fluorescence is normalized relative to that at 0 Zn^{2+} concentration. The intersection of the linear fits to the data yields a dead time of 12 ± 2 ms. Inset: determination of the mixing efficiency by measuring the quenching of tryptophan fluorescence by iodide under the same solvent conditions as used in the refolding experiments on cyt *c* at −35 °C. 56 μM L-tryptophan in the buffer (0.1 M imidazole, pH 6.5) containing 1.5 M GdnHCl and 4.6 M LiCl was mixed at −35 °C with 6 volumes of variable concentrations of NaI in the buffer containing 5.5 M LiCl. The resulting fluorescence changes are shown. The final iodide concentrations are shown at the upside of each curve. The fluorescence is normalized relative to that at 0 iodide concentration. Nearly constant curves show the excellence of the mixing.

Quenching of the fluorescence of L-tryptophan by NaI, a well-characterized process with a bimolecular rate constant of 5×10^9 M^{-1} s^{-1} (*16*), was used for estimation of the mixing efficiency of the instrument. Changes in fluorescence after mixing of a L-tryptophan solution with various concentrations of NaI solutions were followed at −35 °C under exactly the same solvent conditions as used in the present refolding experiments at that temperature in the presence of LiCl. No significant time-dependent changes are seen in the traces, indicating that the mixing is completed within the dead time of the instrument (see inset of Figure 1). The excellence of the mixing efficiency has similarly been verified in mixing solutions under the same conditions as in the present refolding experiments at −20 °C in the presence of ethylene glycol as antifreeze (data not shown).

The binding of 8-hydroquinoline (8-Hq) to Mg^{2+} is a convenient test reaction for the dead time determination of fluorescence stopped-flow experiments at room temperature (*17*). The reaction rate, however, is greatly diminished when the temperature is lowered to −30 °C, so the faster reaction

with Zn^{2+} was used as a test reaction. The reaction of 8-Hq with various excess amounts of Zn^{2+} was measured fluorometrically under basically the same solvent conditions as in the inset. The reaction is pseudo first order, and the logarithmic plots of the fluorescence changes can be fitted to straight lines, yielding a dead time of 12 ± 3 ms (Figure 1). The linearity of the plots provides further confirmation of the high mixing efficiency.

Separate measurements further support this conclusion: 60−76 wt % glycerol solutions in 10 mM Hepes, pH 7.1, containing 7 μM umbelliferone (a fluorescent pH indicator with p$K_a \approx 7.7$) were 1:6 mixed at 20 °C with the same concentrations of glycerol solutions in 10 mM Hepes, pH 8.3, using the stopped-flow instrument. The fluorescence changes of umbelliferone accompanying its diffusion-limited proton-exchange reaction (*18*) with Hepes were measured. No significant mixing inefficiency was detected for mixing solutions ≤70 wt % glycerol [$\eta \leq 25$ cP (*15*)]. This confirms that the mixing efficiency of the solutions studied in the present refolding experiments was excellent because their viscosities were all ≤22 cP at the experimental temperatures.

Refolding Kinetics of Cyt c. Cyt *c* is a protein whose refolding has most extensively been studied as a prototypical system (*19*). The unfolded protein rapidly collapses to form a compact structure during the burst phase of stopped-flow refolding experiments at room temperature (*20*, *21*). The present experiments were carried out in the presence of 0.1 M imidazole at neutral pH to simplify the kinetics by eliminating slowly refolding species with a misligating histidine (*21*, *22*). Under such conditions the refolding kinetics of cyt *c* are basically described by a three-state mechanism (*19*) as shown in Scheme 1. In this scheme U, I_c, and F represent the unfolded state, the compact intermediate, and the folded state, respectively.

Scheme 1

$$U \xrightarrow{\text{burst}} I_c \xrightarrow{\text{fast}} F$$

Since the fluorescence of the sole tryptophan (Trp59) is quenched almost completely by the heme in the folded state but only 30−40% in the unfolded state, its intensity sensitively monitors the compactness of the molecule (*21*). To investigate the burst phase by decelerating its rate, we applied the low-temperature stopped-flow method to cyt *c* refolding in the presence of ∼4.5 M NaCl as antifreeze [the freezing point of 4.5 M NaCl is −23 °C (*12*)]. Kinetic changes in tryptophan fluorescence were traced to monitor the refolding after rapid dilution of GdnHCl-unfolded cyt *c* at decreasing temperatures from 10 °C. As the temperature is lowered, a major exponential refolding phase becomes progressively slower, and the apparent rate of this phase is ∼70-fold slower at −20 °C than at 10 °C. In addition, as seen in Figure 2A, a new kinetic phase (phase II) appears in the kinetics at −20 °C. The time dependence of this phase deviates slightly but significantly from that of the subsequent exponential changes. The burst phase (phase I) and the major exponential phase (phase III) of this trace would correspond to the $U \rightarrow I_c$ and $I_c \rightarrow F$ processes, respectively. Phase IV can be assigned to a minor refolding phase associated with proline cis/trans isomerization (*23*). All phases except for phase II have also been observed at room temperature (*19*, *21*).

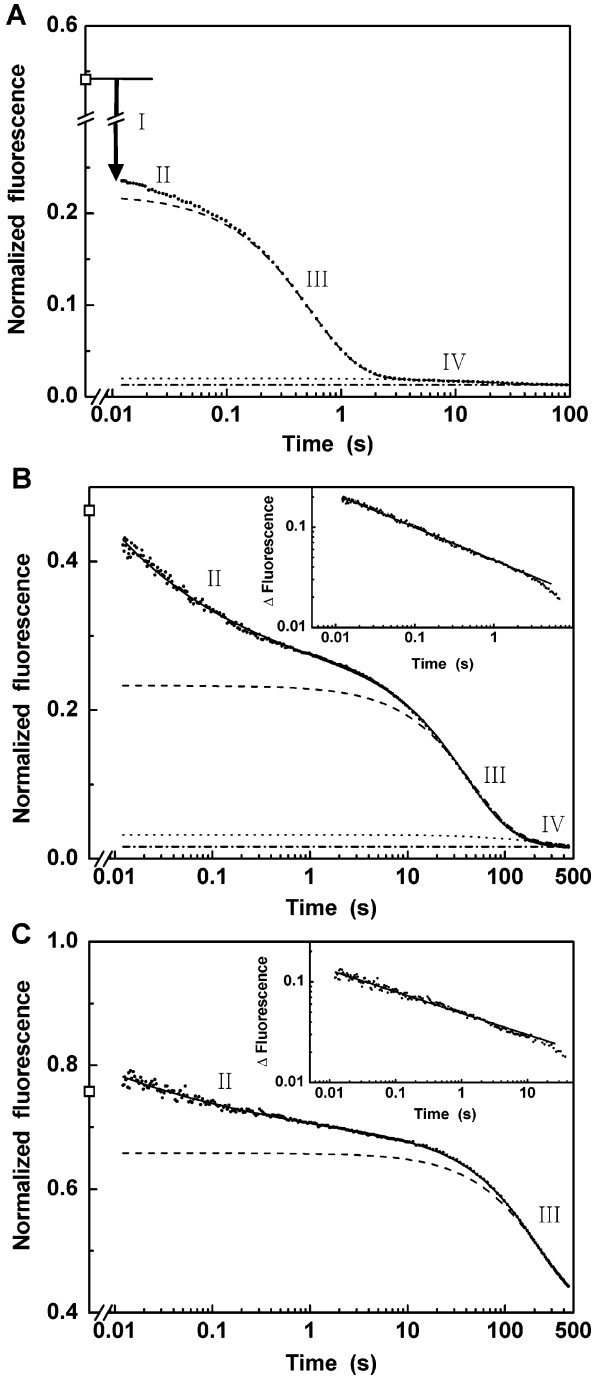

FIGURE 2: Stopped-flow traces of cyt *c* refolding, monitored by tryptophan fluorescence, at pH 6.5, −20 °C, in the presence of 3.6 M NaCl (A) and at pH 6.5, −35 °C, in the presence of 5.4 M LiCl (B) and 5.0 M LiCl (C). The fluorescence is normalized relative to that of the initial states. The symbols (□) indicate the fluorescence of the unfolded protein under the refolding conditions, extrapolated from the unfolded baselines of the equilibrium transition curves. 70 μM cyt *c* in unfolding buffers containing 4.0 M (A) and 1.5 M (B and C) GdnHCl was mixed with 6 volumes of refolding buffers. The final GdnHCl concentrations were 1.2 M (A), 0.21 M (B), and 0.90 M (C). The data for $t \geq 0.3$ s (A), ≥50 s (B), and ≥300 s (C) were fitted to a double, double, and single exponential, respectively. The dashed, dotted, and dash−dotted lines show the best fits, their minor slow components, and final levels, respectively. The solid lines are the fits of the entire kinetics to a power law plus a double (B) or single (C) exponential. Insets: double logarithmic plots of phase II isolated by peeling back the slower exponential phase(s). The solid lines are the fits of the data to straight lines, with slopes of −0.33 (B) and −0.21 (C).

Quantitative analysis of phase II is difficult because of its small amplitude at −20 °C. To further characterize this phase by decelerating its kinetics, the refolding was measured at lower temperatures down to −35 °C in the presence of 5.0−5.4 M LiCl as antifreeze [the freezing point of 5.0 M LiCl is ∼−40 °C (*24*)]. The refolding kinetics in the presence of LiCl above −20 °C were similar in time dependence to those in the presence of NaCl at the corresponding temperatures (data not shown). The phase II amplitude, however, was markedly enhanced below −30 °C. Panels B and C of Figure 2 show the refolding kinetics at −35 °C after denaturant concentration jumps to the folded baseline region and to near the midpoint of the equilibrium unfolding transition, respectively. Three distinct phases (II−IV) are seen in Figure 2B, while the last is not observed in Figure 2C because of its extreme slowness. The major exponential phase (phase III) at this temperature is ∼10^4-fold slower than at 10 °C under the same solvent conditions. Furthermore, phase II seen in both of the panels is highly extended and nonexponential. The amplitudes of this phase, isolated by peeling back the slower exponential phase(s), are shown in the insets as double logarithmic plots. The plots are linear over 2−3 decades in time with slopes of ∼−0.2 to −0.3, indicating that phase II can be well described by a $1/t^n$ power law, where $n < 1$ measures the degree of the nonexponentiality.

The two traces were analyzed more comprehensively by the nonlinear least-squares method, i.e., by fitting the data to the function $f(t) + g(t)$, where $f(t)$ stands for phase II and $g(t)$ for phases III and IV plus an offset. Three types of $f(t)$, namely, a power law having the form $(a/t)^n$ with $n < 1$, a stretched exponential having the form $\exp[-(kt)^\beta]$ with $\beta < 1$, and a multiple exponential, were tested in the fitting (Table 1). Almost equal values for the goodness of fit, χ^2, were obtained by selecting either a power law or a stretched exponential as $f(t)$. At least three exponentials were required to obtain the same quality of fit as with the above two functions, if a multiple exponential was adopted as $f(t)$. It is to be noted that a power law and a stretched exponential have two and three adjustable parameters, respectively, whereas a triple exponential has as many as six, and thus the former two can describe the extended kinetics much more simply than the latter.

A series of kinetic measurements of the refolding at low temperatures were carried out at different final GdnHCl concentrations after mixing. Panels A and B of Figure 3 show the GdnHCl dependence of the cumulative amplitudes for the refolding phases at −20 °C in the presence of high NaCl concentrations and at −35 °C in the presence of high LiCl concentrations, respectively. In the figure are also shown the equilibrium unfolding curves. The final levels of the kinetics are almost in agreement with the equilibrium ones in the pretransition regions, but this was not confirmed in the transition regions because of the extreme slowness of phase IV. Note that the concentrations of antifreeze NaCl and LiCl were not kept constant but decreased linearly with GdnHCl concentration (see Materials and Methods). This is partly because of the solubility limits of the neutral salts in the presence of high GdnHCl concentrations and partly because GdnHCl also serves as antifreeze. Each of the equilibrium curves at −20 and −35 °C can be fitted to a two-state transition model. The transition midpoints at −20 and −35 °C are 2.57 and 0.94 M, respectively, in GdnHCl concentration. The former value is comparable to a midpoint of 2.85 M (*21*) observed at room temperature in the absence of antifreeze, but the latter value is much lower than this value. The lower stability of the F state at −35 °C is primarily due to the presence of a concentrated salting-in agent, LiCl (*25*). On the other hand, the cooperativity indices (m values) of the transitions at −20 and −35 °C are comparable to or somewhat larger than $m = 2.43$ kcal mol^{-1} M^{-1} (*21*) (1 cal = 4.18605 J) at room temperature.

Table 1: Kinetic Parameters for the Refolding of Cyt *c* at −35 °C[a]

[GdnHCl] (M)	$f(t) = (a_3/t)^n$ a_3 (s)	n	χ^{2b}
0.21	5.6×10^{-5}(4)	0.29(1)	1.4×10^{-5}
0.90	2.6×10^{-5}(8)	0.19(1)	1.7×10^{-5}

[GdnHCl] (M)	$f(t) = a_3 \exp[-(k_3 t)^\beta]$ a_3	k_3 (s^{-1})	β	χ^{2b}
0.21	0.58(6)	2.4(9) × 10^2	0.24(2)	1.2×10^{-5}
0.90	≥0.4	≥1 × 10^3	0.15(3)	1.7×10^{-5}

[GdnHCl] (M)	$f(t) = \sum_{i=3}^{5} a_i \exp(-k_i t)$ a_5	k_5 (s^{-1})	a_4	k_4 (s^{-1})	a_3	k_3 (s^{-1})	χ^{2b}
0.21	0.102(3)	33(2)	0.067(3)	5.3(4)	0.033(2)	0.34(4)	1.0×10^{-5}
0.90	0.058(1)	25(1)	0.039(1)	1.3(1)	0.014(2)	0.07(2)	1.7×10^{-5}

[GdnHCl] (M)	$g(t) = \sum_{i=1}^{2} a_i \exp(-k_i t) + a_0$ a_2	k_2 (s^{-1})	a_1	k_1(s^{-1})	a_0	χ^{2b}
0.21	0.21(1)	0.025(1)	0.023(6)	0.001(5)	−0.01(6)	1.4×10^{-5}
0.90	0.260(2)	0.0046(1)			0.392(3)	1.7×10^{-5}
0.21	0.20(1)	0.032(2)	0.05(1)	0.009(2)	0.015(1)	1.2×10^{-5}
0.90	0.270(2)	0.0048(1)			0.411(2)	1.7×10^{-5}
0.21	0.15(3)	0.032(4)	0.09(3)	0.013(3)	0.016(1)	1.0×10^{-5}
0.90	0.271(2)	0.0049(1)			0.414(3)	1.7×10^{-5}

[a] The time-dependent fluorescence changes for the refolding of cyt *c* at final GdnHCl concentrations of 0.21 and 0.90 M (panels B and C of Figure 2, respectively) were fitted to the equation $y(t) = f(t) + g(t)$; $f(t)$ is a function corresponding to phase II; three types of $f(t)$, power-law, stretched exponential, and multiple exponential functions, were examined; $g(t)$ represents an offset plus a double exponential corresponding to phases III and IV. The numbers in parentheses represent the errors of the fitting parameters in the last digits. [b] χ^2 is a measure of the goodness of fit and is defined as $\{\sum_{i=1}^{n}[F(t_i) - y(t_i)]^2\}/(n - n_p)$, where $F(t_i)$, $y(t_i)$, n, and n_p are the data and fitting function at time t_i and the numbers of the data points and fitting parameters, respectively.

The amplitude of phase II is so small at −20 °C that its initial level almost agrees with the cumulative amplitude of phase III. The amplitude of phase II, however, is much larger at −35 °C and comparable to that of the major exponential phase (phase III), not only in the folded baseline region but also in the equilibrium transition region. Note that the phase II amplitude at −35 °C over the entire range of GdnHCl concentration measured accounts almost fully for the "burst-phase" amplitude, i.e., the difference between the fluorescence extrapolated from the unfolded baseline and the cumulative phase III amplitude. This suggests that phases I and II correspond to time-unresolved and resolved fluorescence changes associated with the U → I_c process, respectively. The curves of the cumulative phase III amplitudes at −20 and −35 °C are both sigmoidal and can also be fitted to a two-state transition model. Since phase II is fairly separated in time scale from phase III, the curves should represent the preequilibrium U ↔ I_c transitions. The corresponding curve for cyt *c* refolding at room temperature in

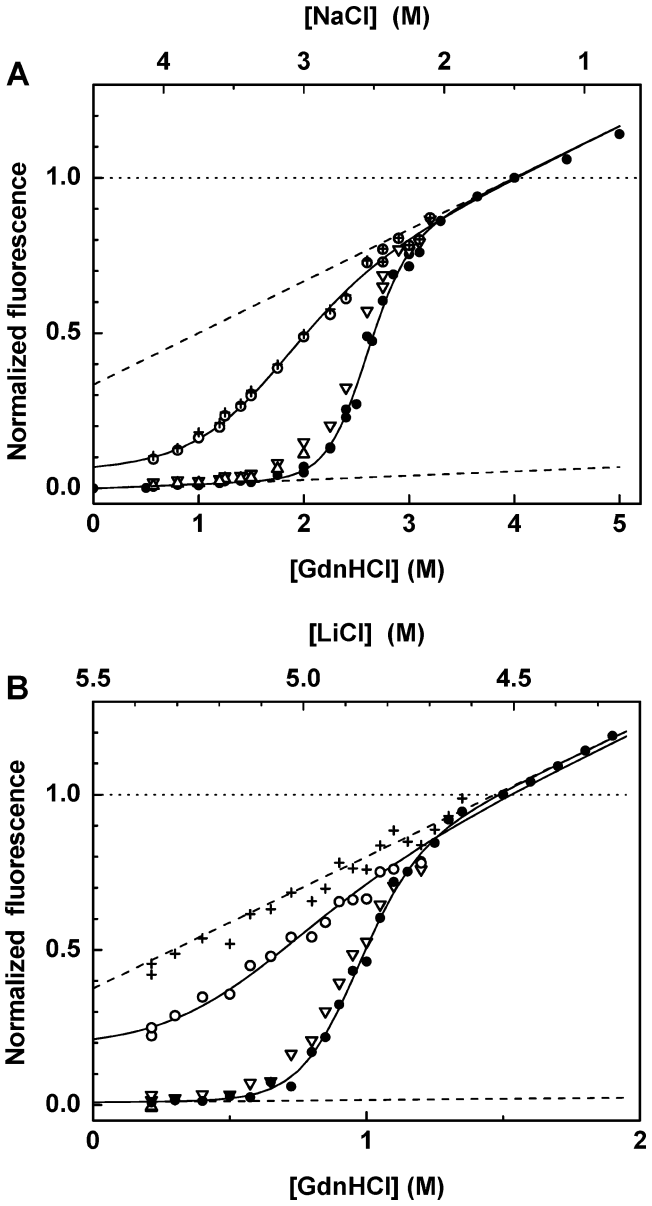

FIGURE 3: Dependence on GdnHCl concentration of the cumulative kinetic amplitudes for the stopped-flow refolding of cyt *c* at pH 6.5, −20 °C, in the presence of NaCl (A) and at pH 6.5, −35 °C, in the presence of LiCl (B). The equilibrium unfolding curves (●) are also shown. The fluorescence is normalized relative to that of the initial states (horizontal dotted lines). 70 μM cyt *c* in unfolding buffers containing 4.0 M (A) and 1.5 M (B) GdnHCl was mixed with 6 volumes of refolding buffers containing different concentrations of GdnHCl. The cumulative amplitudes for phases II (+), III (○), and IV (▽) and the final levels (△), determined from fitting of the refolding kinetics to a power-law decay plus single or double exponential, are shown. The solid lines in each panel are the least-squares fits to the phase III amplitude and equilibrium transition curves to a two-state model with linear dependence of the free energy change on GdnHCl concentration: $-RT \ln K = m(c - c_m)$, where $c_m = 2.6$ M, $m = 2.6$ kcal mol^{-1} M^{-1} (A) and $c_m = 0.94$ M, $m = 4.4$ kcal mol^{-1} M^{-1} (B) for the equilibrium curves, and $c_m = 1.6$ M, $m = 1.1$ kcal mol^{-1} M^{-1} (A) and $c_m = 0.53$ M, $m = 1.8$ kcal mol^{-1} M^{-1} (B) for the amplitude curves. The dashed straight lines are folded and unfolded baselines obtained from fits to the equilibrium curves.

the presence of 0.4 M Na_2SO_4 has similarly been interpreted by Sauder and Roder (*26*).

Refolding Kinetics of Lysozyme. To shed some light on the generality of the occurrence of nonexponential kinetics in the early phases of protein refolding, we have further investigated at low temperatures the refolding of hen egg white lysozyme, another prototypical protein with its well-characterized refolding kinetics. Lysozyme is a globular protein with 129 residues and consists of two subdomains with exclusively α-helical structure (the α-domain) and predominantly β-sheet structure (the β-domain). Stopped-flow fluorescence and continuous-flow small-angle X-ray scattering studies of the refolding of unfolded lysozyme (U) at room temperature have revealed that, like cyt *c*, its initial step is rapid accumulation of a compact intermediate (I_c) occurring in a burst phase completed within the dead time of mixing (*27*). This species has typical properties of the molten globule (*28*). A major population of the I_c state is then transformed into a second intermediate (the I_α state) in a fast phase, and this intermediate is finally converted to the folded state (F) in a slow phase. The I_α state has a nativelike helical structure in the α-domain but remains largely unfolded in the β-domain (*29*). A minor population (~20%) of the I_c state refolds directly to the F state in the fast phase (*30*). Thus overall folding is described as shown in Scheme 2 (*27*, *30*).

Scheme 2

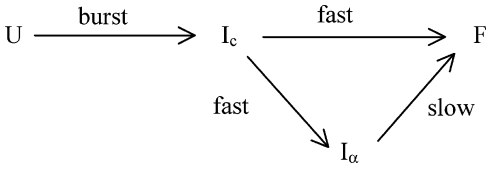

Refolding experiments were carried out by monitoring tryptophan fluorescence changes after stopped-flow dilution of the GdnHCl-unfolded lysozyme at neutral pH and low temperatures in the presence of high NaCl concentrations as antifreeze. Lysozyme molecules in the initial and final states of the experiments are fully unfolded and refolded, respectively, as judged from its fluorescence-monitored unfolding curve at the low temperatures (data not shown). The kinetics at 10 °C were similar in their time dependence to those at room temperature that have been reported earlier (*27*, *30*). A new phase, nonexponential in time course, appeared in the refolding at −10 °C (data not shown), and its amplitude was increased at lower temperatures. Figure 4A shows a typical trace of the refolding at −20 °C in the presence of 3.9 M NaCl. Four distinct phases are seen in the figure. Phases I and II correspond to time-unresolved and resolved portions, respectively, of the burst phase. Thus both of these phases should reflect the U → I_c process. Phases III and IV are exponential phases, both of which are ~2000-fold slower than the respective phases at room temperature. Comparison of the present results with the earlier refolding experiments at room temperature (*27*, *30*) allows to attribute phase III to the $I_c \rightarrow I_\alpha$ and $I_c \rightarrow$ F and phase IV to $I_\alpha \rightarrow$ F processes. Phase II is highly nonexponential and well described by a $1/t^n$ power law (see inset).

To obtain information concerning the role of high NaCl concentrations in the occurrence of the nonexponential refolding kinetics of lysozyme, the kinetics were also measured in the presence of 30−35% (v/v) ethylene glycol as antifreeze instead of high concentrations of NaCl. Figure 4B shows the refolding kinetics of lysozyme at −20 °C after

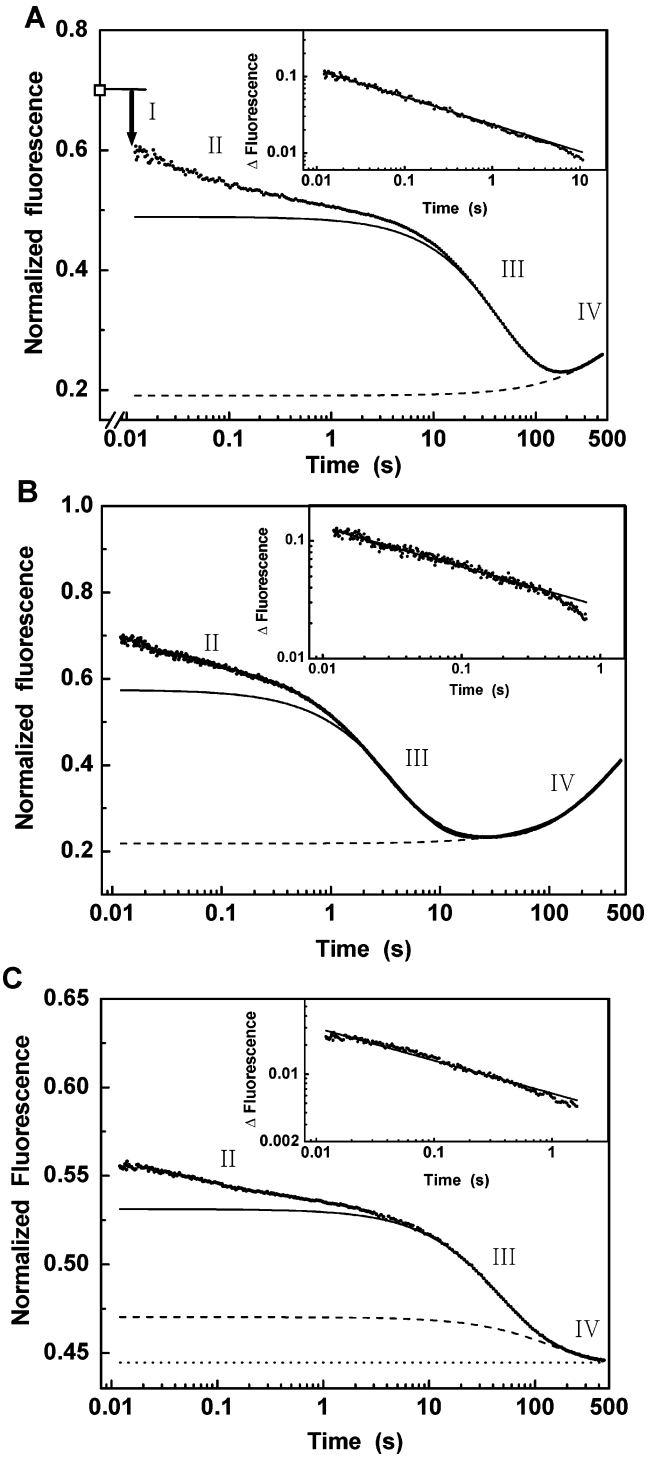

FIGURE 4: Stopped-flow traces of lysozyme refolding, monitored by tryptophan fluorescence, at pH 6.5, −20 °C, in the presence of 3.9 M NaCl (A) and 30% (v/v) ethylene glycol (B) and at pH 1.5, 4.5 °C, in the presence of 70 mM NaCl (C). The fluorescence is normalized similarly to Figure 2. The symbol (□) indicates the fluorescence of the unfolded protein under the refolding conditions, extrapolated similarly to Figure 2. 28−70 μM lysozyme in unfolding buffers containing 5.5 M (A), 5.6 M (B), and 6.0 M (C) GdnHCl was mixed with 6 volumes of refolding buffers. The final GdnHCl concentrations were 0.79 M (A), 0.80 M (B), and 0.86 M (C). The data for $t \geq 30$ s (A), ≥ 1.5 s (B), and ≥ 30 s (C) were fitted to a double exponential, and their best fits, slower components, and final levels are shown by the solid, dashed, and dotted lines, respectively. Insets: double logarithmic plots of phase II isolated by peeling back the slower exponential phases. The solid lines are the fits of the data to straight lines, with slopes of −0.36 (A), −0.34 (B), and −0.34 (C).

GdnHCl dilution in the presence of 30% ethylene glycol. In addition to slow exponential phases (phases III and IV), a faster nonexponential phase (phase II) is seen in the figure, and this phase again follows a power law (see inset).

A similarly nonexponential phase (phase II) was observed in the refolding of lysozyme in 70 mM NaCl at pH 1.5 and 4.5 °C (Figure 4C). Note that the temperature is above 0 °C, so that the presence of antifreeze was not required in this experiment. The experiment was performed under the same conditions as used in the kinetic far-UV CD experiment of lysozyme refolding reported by Ikeguchi et al. (*28*). At the acid pH, the I_α state is destabilized (*31*), and thus the kinetic change following phase II is monotonic in time and can be fitted to the sum of two exponentials with apparent rate constants of $(2.5 \pm 0.1) \times 10^{-2}$ s^{-1} and $(6.9 \pm 0.3) \times 10^{-3}$ s^{-1}, in reasonable agreement with those determined from the CD experiment (3.4×10^{-2} s^{-1} and 6.9×10^{-3} s^{-1}). Phase II was not observed in the CD experiment, which is probably due to its lower amplitude or lower time resolution (order of 1 s) of the experiment.

DISCUSSION

The most significant finding of the present studies is that phase II for cyt *c* and lysozyme refolding at neutral pH is highly nonexponential at low temperatures in the presence of high concentrations of NaCl or LiCl. Highly nonexponential kinetics were also observed for lysozyme refolding at low salt and neutral pH in the presence of ethylene glycol as antifreeze. This indicates that the presence of high concentrations of salt is not essential for the occurrence of the nonexponential kinetics. Similarly, nonexponential kinetics were observed for lysozyme refolding at acid pH even without antifreeze. These results, taken together, suggest that the nonexponential behavior represents an inherent property of the proteins at low temperatures. Protein aggregation as a determinant of the nonexponential behavior is ruled out, because the time courses of phase II for cyt *c* at pH 6.5, −35 °C, and for lysozyme at pH 6.5, −20 °C, and pH 1.5, 4.5 °C, are almost invariant on 3.5−35-fold dilution of protein concentrations (Figure 5).

The significance of the burst phase for protein refolding has been a subject of controversy (*32*), but this phase is usually assumed to reflect the formation of a folding intermediate (*9*−*11*). Using a submillisecond capillary mixing technique monitoring Trp59 fluorescence, Shastry and Roder (*33*) have revealed that the major early phase of cyt *c* refolding at room temperature is a single exponential with a time constant of ∼50 μs. This suggests that a distinct thermodynamic barrier separates the U and I_c states. Lysozyme refolding at room temperature has not been characterized in the submillisecond time frame. The dead time signal changes of tryptophan fluorescence and far-UV CD stopped-flow experiments on the protein, however, gave identical normalized GdnHCl unfolding curves of the I_c state, indicating that the earliest event of the refolding is a cooperative two-state transition between the U and I_c states, separated by an energy barrier (*34*). Thus simple exponential kinetics would be observed if one measures the kinetics of the transition with higher time resolution. On the other hand, the nonexponential refolding kinetics of the two proteins at low temperatures indicate a distribution of the barrier heights between the two

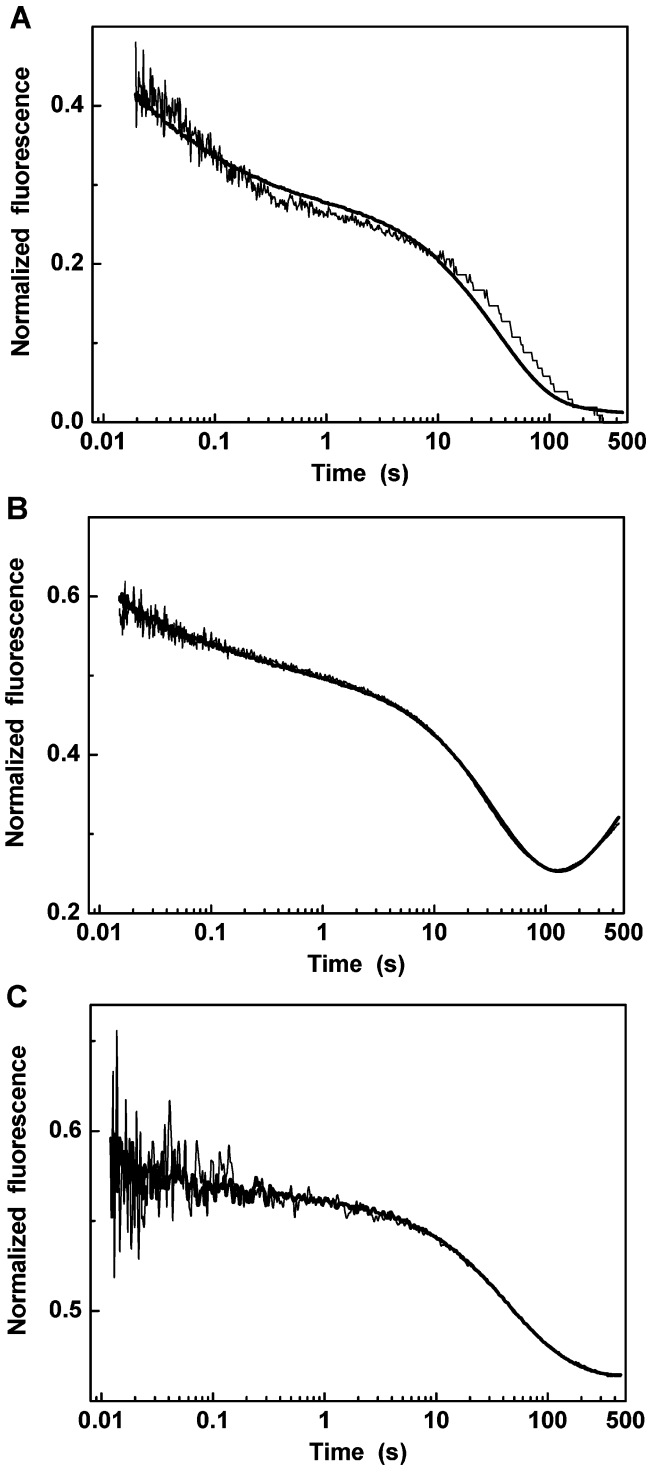

FIGURE 5: Dependence of the refolding kinetics on protein concentrations. Typical kinetic traces are shown for cyt *c* refolding at pH 6.5, −35 °C (A), and for lysozyme refolding at pH 6.5, −20 °C (B), and at pH 1.5, 4.5 °C (C), at the extremes of the protein concentrations. The fluorescence is normalized similarly to Figures 2 and 4. The protein concentrations after mixing were 10 μM (thick line) and 0.29 μM (thin line) (A), 5.0 μM (thick line) and 0.50 μM (thin line) (B), and 4.0 μM (thick line) and 1.1 μM (thin line) (C). For all other experimental conditions, see Figures 2 and 4.

states. Hence, the most plausible explanation for the different kinetics observed at different temperatures is as follows: The U state consists of a large ensemble of unfolded substates U_i ($i = 1$ to n) with various nonnative and native intrachain interactions (*35*). If the interconversions among U_i are faster than the subsequent barrier crossing, all of the substates are

Scheme 3

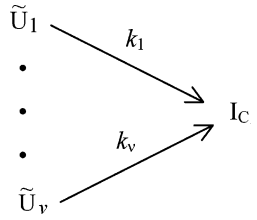

thermally averaged and can be treated as a single state. This simplifies the kinetics of the U→ I_c process, resulting in single-exponential kinetics with an apparent rate constant of $k_{app} = \sum w_i k_i$ (*36*), where w_i and k_i represent the population of U_i relative to the total population of the unfolded state and the rate constant for the $U_i \rightarrow I_c$ process, respectively. Theoretical and computational studies have shown that protein folding can be described as configurational diffusion on an underlying energy landscape. The reconfigurational time τ in a rugged energy landscape has theoretically been shown to have a super-Arrhenius temperature dependence and is given by $\tau = \tau_0 \exp[(\Delta E/k_B T)^2]$ (*2*). The prefactor τ_0 is the time scale of large segmental motions of the chain, and ΔE is the root-mean-square magnitude of the ruggedness having a Gaussian distribution. The ruggedness arises from nonnative interactions or native interactions in wrong topologies. As the temperature decreases, the conformational interconversions among U_i would thus become slower until the protein finally becomes trapped in local energy minima and escape rates from these traps dominate the $U \rightarrow I_c$ process. For instance, for ΔE of 2.5 kcal/mol, the exponential factor increases (2.2×10^4)-fold with a temperature decrease from 25 to −35 °C. At lowered temperatures, the barrier heights of this process therefore vary for different molecules, and its kinetics would be a superposition of many parallel paths with different rates from local minima $\tilde{U}_i$ ($i = 1$ to ν) (see Scheme 3), resulting in nonexponential kinetics describable by a stretched exponential or a power law (*5*, *6*).

Nonexponential kinetics can also be explained by assuming a downhill-folding mechanism (*2*), in which the activation barrier for folding is small or nonexistent. This makes the refolding a noncooperative and gradual process (*37*). Gruebele and co-workers (*8*) interpreted the nonexponential refolding kinetics of two cold-denatured proteins in terms of this mechanism. The interpretation was supported by the findings that the kinetics become exponential at lower temperatures where the folding is less energy biased toward the native state, in accordance with the energy landscape theory (*2*). This is in sharp contrast with the present observation that the early stages of cyt *c* refolding remain highly nonexponential even at the midpoint of the equilibrium transition where there is no native free energy bias. Furthermore, the sharpness of the GdnHCl unfolding transition of the I_c state in lysozyme under the same conditions as in Figure 4A, i.e., at −20 °C in the presence of ∼4 M NaCl, is almost the same (data not shown) as that of the transition at room temperature (*34*), suggesting that the transition at the low temperature is also a barrier-crossing process. Interpretation of the nonexponential refolding behavior at the low temperatures in terms of the downhill-folding mechanism is therefore unlikely to be relevant to both cyt *c* and lysozyme.

Analytical theory (*2*, *4*) and lattice (*5*) and off-lattice (*6*) simulations show that the folding kinetics of protein-like

heteropolymers become glassy and nonexponential near or below a critical low temperature denoted as glass transition temperature T_g. A useful strategy of designing good folding sequences is to maximize the gradient-to-ruggedness ratio of the folding landscape, and this ratio can be quantified by the ratio T_f/T_g (*2*, *4*, *6*), where T_f is the folding temperature at which the occupation of the folded state is 50%. The nonexponential kinetics described in this paper probably correspond to the glassy behavior of folding proteins and suggest that $T_g \geq -35$ and -20 °C for cyt *c* and lysozyme, respectively, at neutral pH. These relations lead to $T_f/T_g \leq 1.6$ for cyt *c* and $T_f/T_g \leq 1.5$ for lysozyme under the plausible assumption that $T_f \leq 100$ °C for these proteins (*38*). These relations are consistent with a theoretical estimate of $T_f/T_g \approx 1.6$ for a realistic folding funnel of a fast-folding protein (*39*) and suggest that the folding funnels of the proteins are moderately rugged in the upper portions.

NMR spectroscopy of hen lysozyme has shown that nativelike extensive clusters of hydrophobic residues involving its six tryptophans exist within the protein even under strongly denaturing conditions (*40*, *41*). The mechanism by which the early phases of lysozyme refolding at pH 1.5 are nonexponential and glassy even at temperatures as high as 4.5 °C is unknown but may involve changes in the folding landscape of the protein due to perturbation of such nativelike interactions by the acid pH.

In summary, low-temperature stopped-flow studies of the early phases of cyt *c* and lysozyme refolding have revealed highly nonexponential kinetics. Our findings suggest that the early-phase kinetics of these proteins are dominated at low temperatures by ruggedness in the upper regions of the folding energy landscapes. This is consistent with the view that the evolution has engineered proteins that are foldable within a biologically relevant time by optimizing the energy bias toward the native state while minimizing the landscape ruggedness to a required extent (*2*).

ACKNOWLEDGMENT

We thank Mitsunori Takano and Hironori K. Nakamura for helpful discussions and Jeremy Tame for valuable comments on the manuscript.

REFERENCES

1. Levinthal, C. (1969) in *Mössbauer Spectroscopy in Biological Systems. Proceedings of a Meeting Held at Allerton House, Monticello, Illinois* (Debrunner, P., Tsibris, J., and Munck, E., Eds.) pp 22−24, University of Illinois Press, Urbana, IL.
2. Bryngelson, J. D., Onuchic, J. N., Socci, N. D., and Wolynes, P. G. (1995) *Proteins: Struct., Funct., Genet. 21*, 167195.
3. Dill, K. A., and Chan, S. (1997) *Nat. Struct. Biol. 4*, 10−19.
4. Onuchic, J. N., Luthey-Shulten, Z., and Wolynes, P. G. (1997) *Annu. Rev. Phys. Chem. 48*, 545−600.
5. Socci, N. D., Onuchic, J. N., and Wolynes, P. G. (1998) *Proteins: Struct., Funct., Genet. 32*, 136−158.
6. Nymeyer, H., Garćia, A. E., and Onuchic, J. N. (1998) *Proc. Natl. Acad. Sci. U.S.A. 95*, 5921−5928.
7. Gillespie, B., and Plaxco, K. W. (2000) *Proc. Natl. Acad. Sci. U.S.A. 97*, 12014−12019.
8. Sabelko, J., Ervin, J., and Gruebele, M. (1999) *Proc. Natl. Acad. Sci. U.S.A. 96*, 6031−6036.
9. Roder, H., and Colón, W. (1997) *Curr. Opin. Struct. Biol. 7*, 15−28.
10. Clarke, A. R., and Waltho, J. P. (1997) *Curr. Opin. Biotechnol. 8*, 400−410.
11. Arai, M., and Kuwajima, K. (2000) *Adv. Protein Chem. 53*, 209−282.
12. Auld, D. S. (1979) *Methods Enzymol. 61*, 318−335.
13. Van Wart, H. E., and Zimmer, J. (1981) *Anal. Biochem. 117*, 410−418.
14. Inada, Y., Funahashi, S., and Ohtaki, H. (1994) *Rev. Sci. Instrum. 65*, 18−24.
15. Wolf, A. V., Brown, M. G., and Prentiss, P. G. (1988) in *CRC Handbook of Chemistry and Physics* (Weast, R. C., Astle, M. J., and Beyer, W. H., Eds.) pp D219−D269, CRC Press, Boca Raton, FL.
16. Lehrer, S. S. (1971) *Biochemistry 10*, 3254−3263.
17. Brissette, P., Ballou, D. P., and Massey, V. (1989) *Anal. Biochem. 181*, 234−238.
18. Eigen, M., Kruse, W., Maass, G., and DeMayer, L. (1964) *Prog. React. Kinet. 2*, 287−318.
19. Shastry, M. C. R., Sauder, J. M., and Roder, H. (1998) *Acc. Chem. Res. 31*, 717−725.
20. Pollack, L., Tate, M. W., Darnton, N. C., Knight, J. B., Gruner, S. M., Eaton, W. A., and Austin, R. H. (1999) *Proc. Natl. Acad. Sci. U.S.A. 96*, 10115−10117.
21. Chan, C.-K., Hu, Y., Takahashi, S., Rousseau, D. L., Eaton, W. A., and Hofrichter, J. (1997) *Proc. Natl. Acad. Sci. U.S.A. 94*, 1779−1784.
22. Brems, D. N., and Stellwagen, E. (1983) *J. Biol. Chem. 258*, 3655−3660.
23. Ridge, J. A., Baldwin, R. L., and Labhardt, A. M. (1981) *Biochemistry 20*, 1622−1630.
24. Moran, H. E. (1956) *J. Phys. Chem. 60*, 1666−1667.
25. Nandi, P. K., and Robinson, D. R. (1972) *J. Am. Chem. Soc. 94*, 1299−1308.
26. Sauder, J. M., and Roder, H. (1998) *Folding Des. 3*, 293−301.
27. Segel, D. J., Eliezer, D., Uversky, V., Fink, A. L., Hodgson, K. O., and Doniach, S. (1999) *J. Mol. Biol. 288*, 489−499.
28. Ikeguchi, M., Kuwajima, K., Mitani, M., and Sugai, S. (1986) *Biochemistry 25*, 6965−6972.
29. Radford, S. E., Dobson, C. M., and Evans, P. A. (1992) *Nature 358*, 302−307.
30. Kiefhaber, T. (1995) *Proc. Natl. Acad. Sci. U.S.A. 92*, 9029−9033.
31. Chaffotte, A. F., Guillou, Y., and Goldberg, M. E. (1992) *Biochemistry 31*, 9694−9702.
32. Krantz, B. A., Mayne, L., Rumbley, J., Englander, S. W., and Sosnick, T. R. (2002) *J. Mol. Biol. 324*, 359−371.
33. Shastry, M. C. R., and Roder, H. (1998) *Nat. Struct. Biol. 5*, 385−392.
34. Bachmann, A., Segel, D., and Kiefhaber, T. (2002) *Biophys. Chem. 96*, 141−151.
35. Smith, L. J., Fiebig, K. M., Schwalbe, H., and Dobson, C. M. (1996) *Folding Des. 1*, 95−106.
36. Zwanzig, R., Szabo, A., and Bagchi, B. (1992) *Proc. Natl. Acad. Sci. U.S.A. 89*, 20−22.
37. Muñoz, V. (2002) *Int. J. Quantum Chem. 90*, 1522−1528.
38. Privalov, P. L., and Khechinashvili, N. N. (1974) *J. Mol. Biol. 86*, 665−684.
39. Onuchic, J. N., Wolynes, P. G., Luthey-Schulten, Z., and Socci, N. D. (1995) *Proc. Natl. Acad. Sci. U.S.A. 92*, 3626−3630.
40. Schwalbe, H., Fiebig, K. M., Bucks, M., Jones, J. A., Grimshaw, S. B., Spencer, A., Glaser, S. J., Smith, L. J., and Dobson, C. M. (1997) *Biochemistry 36*, 8977−8991.
41. Klein-Seetharaman, J., Oikawa, M., Grimshaw, S. B., Wirmer, J., Duchardt, E., Ueda, T., Imoto, T., Smith, L. J., Dobson, C. M., and Schwalbe, H. (2002) *Science 295*, 1719−1722.

BI034484Y